Vesicle−Biopolymer Gels: Networks of Surfactant Vesicles Connected by Associating Biopolymers

Jae-Ho Lee,[†] John P. Gustin,[†] Tianhong Chen,[‡] Gregory F. Payne,[‡] and Srinivasa R. Raghavan*,[†]

Department of Chemical Engineering, University of Maryland, College Park, Maryland 20742-2111, and Center for Biosystems Research, University of Maryland Biotechnology Institute, College Park, Maryland 20742-4450

Received July 19, 2004. In Final Form: September 30, 2004

The effect of adding an associating biopolymer to surfactant vesicles and micelles is studied using rheology and small-angle neutron scattering (SANS). The associating polymer is obtained by randomly tethering hydrophobic alkyl chains to the backbone of the polysaccharide, chitosan. Adding this polymer to surfactant vesicles results in a *gel*; that is, the sample transforms from a Newtonian liquid to an elastic solid having frequency-independent dynamic shear moduli. SANS shows that the vesicles remain intact within the gel. The results suggest a gel structure in which the vesicles are connected by polymer chains into a three-dimensional network. Vesicle−polymer binding is expected to occur via the insertion of polymer hydrophobes into the vesicle bilayer. Each vesicle thus acts as a multifunctional junction in the network structure. Significantly, gel formation does not occur with the native chitosan that has no hydrophobes. Moreover, adding the hydrophobically modified chitosan to a viscous sample containing wormlike micelles increases the viscosity further but does not give rise to a gel-like response. Thus, the formation of a robust gel network requires both the presence of hydrophobes on the polymer *and* vesicles in solution.

Introduction

Vesicles are hollow spherical structures formed by the self-assembly of surfactants, lipids, or block copolymers in aqueous solution.[1−3] They have long been a scientific curiosity because of their structural resemblance to primitive biological cells. More importantly, vesicles are of technological interest for applications ranging from drug delivery and controlled release to bioseparations and sensing.[1] Many of these applications rely upon the ability of vesicles to entrap desired chemicals in their interior and thereafter release these chemicals to the external medium in a controlled manner.

The term "associating polymer" generally refers to a water-soluble polymer bearing hydrophobic groups either at the chain ends or along the backbone. Such polymers are now widely used in coatings and paints, and the microstructures formed by these polymers in solution have been investigated in detail.[4−6] It is believed that interactions between polymer hydrophobes leads to a transient macromolecular network, thereby imparting significant viscoelasticity to the solution. The interaction of associating polymers with surfactants has also been studied extensively.[5,6] At low surfactant concentrations, the surfactant facilitates the formation of network cross-links and thus enhances the viscosity.[5,6] The formation of spherical micelles at higher surfactant concentrations causes a drop in viscosity due to the "capture" of hydrophobes by the micelles. On the other hand, interactions between wormlike micelles and associative polymers tend to be cooperative, and the viscosity rises.[6] A coherent picture thus exists for the interaction of associating polymers with micelles.

Much less is known, in contrast, about the interactions of associating polymers with vesicles. Such systems are especially complex when the polymer is a hydrophobically modified *polyelectrolyte* and the vesicles also bear charge.[7−13] Polymer−vesicle interactions in such cases will be mediated by a combination of hydrophobic and electrostatic forces. One possible outcome is for the polymer chains to adsorb on the vesicles and act as a stabilizing agent.[8] Alternately, the polymer can cause vesicle fusion or disruption of the bilayer structure. In some cases, the addition of polymer can give rise to faceted vesicles, in contrast to spherical structures.[9] Finally, and most relevant to the present study, the addition of an associating polymer can result in a "vesicle gel", where adjacent vesicles are bridged by polymer chains.[10−14] So far, studies on vesicle gels have largely been carried out with synthetic associative polymers, obtained typically by attaching hydrophobic moieties to water-soluble synthetic polymers such as poly(ethylene oxide) or polyacrylamide.

In this study, we investigate the addition of a hydrophobically modified biopolymer to surfactant vesicles and

* Corresponding author. E-mail: sraghava@eng.umd.edu.
[†] University of Maryland.
[‡] University of Maryland Biotechnology Institute.

(1) Lasic, D. D. *Liposomes: From Physics to Applications*; Elsevier: Amsterdam, 1993.
(2) Kaler, E. W.; Murthy, A. K.; Rodriguez, B. E.; Zasadzinski, J. A. N. *Science* **1989**, *245*, 1371.
(3) Discher, D. E.; Eisenberg, A. *Science* **2002**, *297*, 967.
(4) English, R. J.; Raghavan, S. R.; Jenkins, R. D.; Khan, S. A. *J. Rheol.* **1999**, *43*, 1175.
(5) Annable, T.; Buscall, R.; Ettelaie, R.; Shepherd, P.; Whittlestone, D. *Langmuir* **1994**, *10*, 1060.
(6) Panmai, S.; Prud'homme, R. K.; Peiffer, D. G. *Colloids Surf., A* **1999**, *147*, 3.
(7) Kevelam, J.; vanBreemen, J. F. L.; Blokzijl, W.; Engberts, J. *Langmuir* **1996**, *12*, 4709.
(8) Murphy, A.; Hill, A.; Vincent, B. *Ber. Bunsen-Ges. Phys. Chem. Chem. Phys.* **1996**, *100*, 963.
(9) Regev, O.; Marques, E. F.; Khan, A. *Langmuir* **1999**, *15*, 642.
(10) Loyen, K.; Iliopoulos, I.; Audebert, R.; Olsson, U. *Langmuir* **1995**, *11*, 1053.
(11) Meier, W.; Hotz, J.; GuntherAusborn, S. *Langmuir* **1996**, *12*, 5028.
(12) Marques, E. F.; Regev, O.; Khan, A.; Miguel, M. D.; Lindman, B. *Macromolecules* **1999**, *32*, 6626.
(13) Ashbaugh, H. S.; Boon, K.; Prud'homme, R. K. *Colloid Polym. Sci.* **2002**, *280*, 783.
(14) Antunes, F. E.; Marques, E. F.; Gomes, R.; Thuresson, K.; Lindman, B.; Miguel, M. G. *Langmuir* **2004**, *20*, 4647.

10.1021/la048194+ CCC: $30.25
Published on Web 12/03/2004

micelles. The biopolymer is the polysaccharide, chitosan, which is positively charged at acidic pH.[15] We attach *n*-dodecyl tails ("stickers") to the chitosan backbone so as to obtain an associating biopolymer. We then show that the addition of this polymer to positively charged surfactant vesicles results in the formation of vesicle gels. Through the use of small-angle neutron scattering (SANS), we establish that the vesicles remain intact within the gels. We view these vesicle gels as an unusual type of self-assembled, soft material, with potential uses in controlled release applications.[16,17] The gelation of vesicles can be considered a means of entrapping and locking-in the vesicles within a soft matrix. Our use of an associating biopolymer is a step toward ensuring the biocompatibility of candidate systems for drug delivery.[17]

The unique features of chitosan and its derivatives are worth mentioning here. Chitosan is a linear polysaccharide obtained by the partial deacetylation of chitin, a natural polysaccharide next only to cellulose in abundance.[15] Both chitosan as well as its hydrophobically modified counterparts have been finding uses in pharmaceutical applications.[15,17,18] For example, the biocompatibility and antibacterial properties of chitosan derivatives have led to their use in biodegradable wound dressings and sutures. Hydrophobically modified derivatives of chitosan can be synthesized relatively easily and under mild conditions.[19,20] The synthesis of such value-added functional polymers from chitosan and other polysaccharides has been of interest to us.[21,22] Our interest has been partly motivated by environmental issues, because chitosan and chitin are usually obtained from food-processing wastes (crab, shrimp, or lobster shells), generated by the seafood industry in Maryland and elsewhere.[15]

Materials And Methods

Chitosan. Chitosan of medium molecular weight (190−310K) and Brookfield viscosity of 286 cps was obtained from Aldrich. The reported degree of deacetylation was about 80%, and this has been verified by NMR.[23] The chitosan backbone is thus mostly composed of D-glucosamine [β-(1,4)-2-deoxy-2-amino-D-glucopyranose) sugars, with a small fraction of *N*-acetyl-D-glucosamine [β-(1,4)-2-deoxy-2-acetamido-D-glucopyranose] sugars as well. Chitosan is pH-sensitive as a result of its amine groups and is soluble only under acidic conditions, that is, at a pH < 6.5. We have used 1% acetic acid to control the pH in chitosan solutions.[24] Chitosan acts as a cationic polyelectrolyte under these conditions.

Synthesis of Hydrophobically Modified Chitosan (hm-Chitosan). We attached *n*-dodecyl tails to chitosan by reacting the amine groups with *n*-dodecyl aldehyde. All reagents for the synthesis were obtained from Aldrich. The procedure follows that reported in the literature.[19,20] Briefly, it involves the addition of aldehyde to an acidic chitosan solution in a water−ethanol mixture, followed by addition of sodium cyanoborohydride. The molar ratio of aldehyde to that of the chitosan monomer(s) was fixed at 2.5% in this study. The hm-chitosan was precipitated by raising the pH and adding ethanol, and the precipitate was purified by washing with ethanol followed by deionized water. The final hm-chitosan precipitate was redissolved in acetic acid solution, and the concentration was recalibrated. This solution was highly viscous as a result of associations between the hydrophobes. NMR studies on the hm-chitosan[20,23] indicated that the degree of hydrophobic substitution was close to that expected from the reaction stoichiometry (2.5 mol %). Similar results have been reported by others.[24,25] The structure of the hm-chitosan is schematically illustrated in Figure 1.

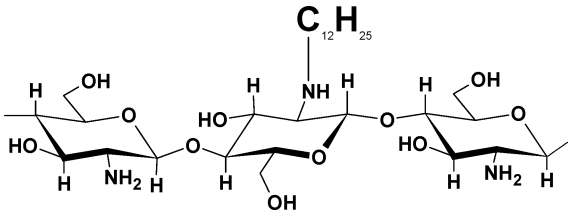

Figure 1. Chemical structure of hm-chitosan with C_{12} hydrophobes.

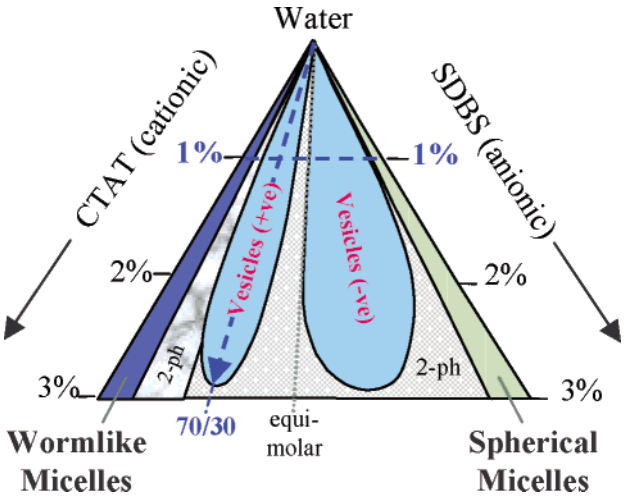

Figure 2. Water-rich corner of the CTAT/SDBS/water ternary phase diagram, redrawn from ref 26. All concentrations are expressed in weight percent. The focus of this study is on the wormlike micelle and vesicle phases rich in CTAT. In the vesicle region, a 70:30 CTAT/SDBS weight ratio, marked by the dashed arrow, was the composition of choice. Systematic studies as a function of CTAT/SDBS ratio were conducted at an overall concentration of 1 wt %, shown by the dashed horizontal line.

Surfactant Vesicles and Micelles. The surfactant system employed was a mixture of the cationic surfactant, cetyl trimethylammonium tosylate (CTAT), and the anionic surfactant, sodium dodecyl benzene sulfonate (SDBS).[2,26] The surfactants were purchased from Aldrich, and all solutions were made using distilled−deionized water. The phase diagram for CTAT/SDBS mixtures has been reported previously,[26] and the water-rich corner is redrawn in Figure 2. Rodlike or wormlike micelles (M) are present in the CTAT-rich corner, and unilamellar vesicles (V) are present in the two lobes extending from the water corner. The left-hand lobe corresponds to CTAT-rich or cationic vesicles, and our attention was primarily focused on these compositions.

Sample Preparation and Phase Characterization. Surfactant and polymer mixtures of desired composition were prepared by mixing the corresponding stock solutions. Samples were mildly heated at 50 °C for 2 h, followed by centrifugation to remove bubbles. The sol−gel phase boundary was evaluated visually by tube inversion (details under Results). For SANS experiments, the samples were prepared in D_2O, obtained from

(15) Skjak-Braek, G.; Anthonsen, T.; Sandford, P. *Chitin and Chitosan: Sources, Chemistry, Biochemistry, Physical Properties, and Applications*; Elsevier: London, 1988.
(16) Kim, M. K.; Chung, S. J.; Lee, M. H.; Cho, A. R.; Shim, C. K. *J. Controlled Release* **1997**, *46*, 243.
(17) Uchegbu, I. F.; Schatzlein, A. G.; Tetley, L.; Gray, A. I.; Sludden, J.; Siddique, S.; Mosha, E. *J. Pharm. Pharmacol.* **1998**, *50*, 453.
(18) Sihorkar, V.; Vyas, S. P. *J. Pharm. Pharm. Sci.* **2001**, *4*, 138.
(19) Yalpani, M.; Hall, L. D. *Macromolecules* **1984**, *17*, 272.
(20) Desbrieres, J.; Martinez, C.; Rinaudo, M. *Int. J. Biol. Macromol.* **1996**, *19*, 21.
(21) Chen, T. H.; Kumar, G.; Harris, M. T.; Smith, P. J.; Payne, G. F. *Biotechnol. Bioeng.* **2000**, *70*, 564.
(22) Aberg, C. M.; Chen, T. H.; Olumide, A.; Raghavan, S. R.; Payne, G. F. *J. Agric. Food Chem.* **2004**, *52*, 788.
(23) Lee, J.-H. Ph.D. Dissertation, University of Maryland, College Park, MD, 2004.
(24) Kjoniksen, A. L.; Iversen, C.; Nystrom, B.; Nakken, T.; Palmgren, O. *Macromolecules* **1998**, *31*, 8142.
(25) Esquenet, C.; Terech, P.; Boue, F.; Buhler, E. *Langmuir* **2004**, *20*, 3583.
(26) Koehler, R. D.; Raghavan, S. R.; Kaler, E. W. *J. Phys. Chem. B* **2000**, *104*, 11035.

Cambridge Isotopes. The hm-chitosan was vacuum-dried before solubilization in D_2O.

Dynamic Light Scattering (DLS). Vesicle solutions were studied at 25°C using DLS. A Photocor-FC light scattering instrument with a 5-mW laser light source at 633 nm was used, with the scattering angle being 90°. A logarithmic correlator was used to obtain the autocorrelation function, which was analyzed by the method of cumulants to yield a diffusion coefficient.[27] The apparent hydrodynamic size of the vesicles was obtained from the diffusion coefficient through the Stokes−Einstein relationship.[27]

Rheological Studies. Steady and dynamic rheological experiments were performed on a Rheometrics RDA III strain-controlled rheometer. A cone-and-plate geometry of 50-mm diameter and with a 0.04-rad cone angle was used. Dynamic frequency spectra were obtained in the linear viscoelastic regime of the samples, as determined by dynamic strain sweep experiments.

SANS. SANS measurements were made on the NG-3 (30 m) and NG-1 (8 m) beamlines at the National Institute of Standards and Technology (NIST) in Gaithersburg, MD. Samples were studied at 25 °C in 2-mm quartz cells. The scattering spectra were corrected and placed on an absolute scale using calibration standards provided by NIST. The data are shown for the radially averaged, absolute intensity I versus the scattering vector $q = (4\pi/\lambda)\sin(\theta/2)$, where λ is the wavelength of incident neutrons and θ is the scattering angle.

SANS Modeling. The SANS intensity $I(q)$ can be modeled purely in terms of the form factor $P(q)$ of scattering particles when the particles are noninteracting, that is, when the structure factor $S(q) \rightarrow 1$. The form factor $P(q)$ for scattering from unilamellar vesicles of radius R and bilayer thickness t is given by the following expression:[28,29]

$$P(q) = (\Delta\rho)^2\left\{\frac{4}{3}\pi R^3\frac{3J_1(qR)}{qR} - \frac{4}{3}\pi(R+t)^3\frac{3J_1[q(R+t)]}{q(R+t)}\right\}^2 \quad (1)$$

where $(\Delta\rho)$ is the difference in scattering length density between the vesicle bilayer and the solvent. $(\Delta\rho)^2$ is thus a measure of the scattering contrast. $J_1(x)$ is the first-order Bessel function, given by

$$J_1(x) = \frac{\sin x - x\cos x}{x^2} \quad (2)$$

For thin bilayers ($t \ll R$), or equivalently for large vesicles, $P(q)$ reduces to the following expression:

$$P(q) = (\Delta\rho)^2(4\pi R)^2\frac{t^2}{q^2}\sin^2(qR) \quad (3)$$

Equation 3 indicates that, for large, noninteracting vesicles, $I(q)$ should show a q^{-2} decay in the low-q range.

If the vesicles are polydisperse, the form factor has to be averaged over the vesicle distribution in the following manner:[28,29]

$$P(q) = \int f(R)\,P(q,R)\,\mathrm{d}R \quad (4)$$

where $P(q, R)$ is the form factor for a vesicle of radius R (eq 1). The polydispersity in vesicle radius $f(R)$ can be accounted for by a Schultz distribution:

$$f(R) = \left(\frac{p+1}{R_0}\right)^{p+1}\frac{R^p}{\Gamma(p+1)}\exp\left[-(p+1)\frac{R}{R_0}\right] \quad (5)$$

In the above expression, R_0 is the average vesicle radius and p is the polydispersity index. The latter is related to the spread of the radius distribution by

$$\sigma_R = \frac{\Delta R}{R_0} = \frac{1}{\sqrt{p+1}} \quad (6)$$

Results

We performed our initial studies with CTAT/SDBS solutions at a total surfactant concentration of 1 wt %, indicated in Figure 2 by a dashed horizontal line. Samples with various weight ratios of CTAT to SDBS along this line were prepared. When the hm-chitosan was added to samples rich in the anionic surfactant, SDBS, a precipitate was obtained. The structure of the precipitate is the subject of ongoing study and will not be discussed here. Our focus will be restricted to compositions rich in the cationic surfactant, CTAT, that is, those compositions to the left of the equimolar line in Figure 2. Within this composition range, samples in the CTAT-rich corner (CTAT/SDBS weight ratios from 100:0 to about 91:9) consist of rodlike or wormlike micelles. For slightly higher SDBS content (CTAT/SDBS ratios around 70:30), unilamellar vesicles spontaneously form at equilibrium. Note that these micelles and vesicles both bear a positive charge due to an excess of CTAT. The weight ratio of 70:30 CTAT/SDBS (ca. 2:1 molar ratio) falls in the middle of the vesicle lobe, and we fixed this composition for the majority of our vesicle studies.

The addition of hm-chitosan has different but related effects on CTAT/SDBS micelles and vesicles. The micelle case is discussed in detail later but will be briefly stated here. Consider a sample containing 1% CTAT, which is clear, colorless, and slightly viscous due to the presence of entangled wormlike micelles. Upon adding 0.55% hm-chitosan, the sample becomes perceptibly more viscous (see Figure 9 later) while remaining clear and colorless. Now, consider instead a 1% mixture of CTAT/SDBS at a 70:30 weight ratio. This sample is located in the vesicle lobe and is a nonviscous, bluish solution, reflecting the presence of unilamellar vesicles (Figure 3a). DLS measurements reveal that the vesicle diameter is approximately 120 nm in this sample. When 0.55% hm-chitosan is added, the sample is instantaneously transformed into an elastic gel that is able to hold its own weight in the vial (Figure 3a). Thus, the mixture of the nonviscous vesicle solution with a small amount of hm-chitosan results in a gel. Interestingly, as seen in Figure 3a, the gel has the same bluish color as does the vesicle solution. We will presently discuss the rheology of these vesicle−polymer gels in detail.

Phase Behavior and Rheology of Vesicle−Polymer Mixtures. We studied numerous vesicle−polymer mixtures to map out the rheological "phase diagram" shown in Figure 3b. This is a plot of hm-chitosan concentration against total surfactant concentration, with the surfactant ratio fixed at 70:30 CTAT/SDBS. The path of increasing surfactant at this ratio is indicated on the phase diagram (Figure 2) by a dashed line. Figure 3b shows a sol−gel phase boundary demarcated by tube inversion experiments. Tube inversion is frequently employed in studying gels and is basically a measure of sample yield stress.[30] Thus, a gel-like sample with sufficient yield stress will be able to hold its own weight in an inverted vial (Figure 3a), whereas a viscous sol with a nonexistent or low yield stress will drop down. We employed the same amount of sample in identical vials for the tube inversion experiments and

(27) Brown, W. *Dynamic Light Scattering: The Method and Some Applications*; Clarendon Press: Oxford, 1993.

(28) *Small-Angle X-Ray Scattering*; Glatter, O., Kratky, O., Eds.; Academic Press: New York, 1982.

(29) *Neutron, X-Ray and Light Scattering: Introduction to an Investigative Tool for Colloidal and Polymeric Systems*; Zemb, T., Lindner, P., Eds.; Elsevier: Amsterdam, 1991.

(30) Li, H.; Yu, G. E.; Price, C.; Booth, C.; Hecht, E.; Hoffmann, H. *Macromolecules* **1997**, *30*, 1347.

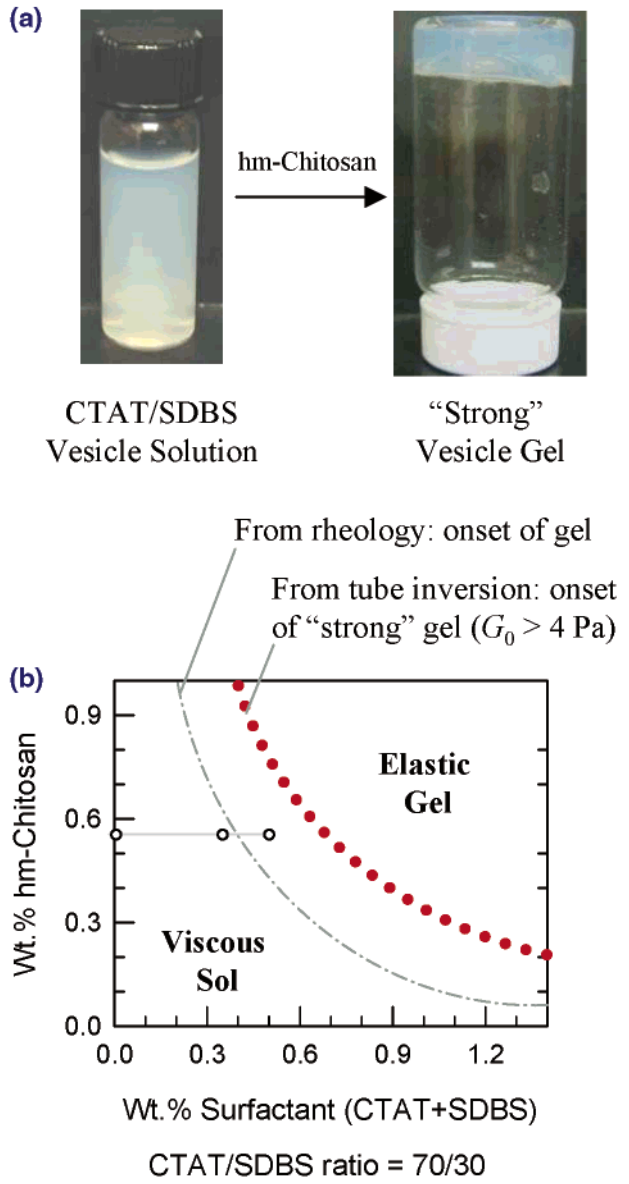

Figure 3. (a) Photograph of a CTAT/SDBS vesicle solution before and after addition of hm-chitosan. The polymer transforms the vesicle solution into an elastic gel that is able to hold its own weight in the inverted vial. (b) Phase map of the hm-chitosan/vesicle system showing the sol−gel boundary obtained by tube inversion experiments. This boundary separates samples that are viscous sols from those that are strong elastic gels. An approximate boundary estimated from rheological data, corresponding to the onset of a weak gel (nonzero equilibrium modulus), is also indicated. Dynamic rheological data for the samples marked by unfilled circles are shown in Figure 4

observed each sample for several minutes after inversion. As will be shown by rheological measurements, the boundary from tube inversion corresponds to the onset of a "strong" gel, with a modulus around 4 Pa. The boundary represents an inverse relationship between the polymer and the vesicle concentrations. This implies that the onset of a gel requires both a critical vesicle as well as a critical polymer concentration.

The onset of gelation was then studied using dynamic rheology. Figure 4 compares the frequency response of four samples with identical hm-chitosan concentrations of 0.55%. The first sample contains no surfactant, and the remaining three are vesicle samples (70:30 CTAT/SDBS) with varying surfactant concentrations. The data shows the elastic modulus G' and the viscous modulus G'' as functions of the angular frequency ω. The 0.55% polymer solution is a Newtonian fluid with a viscosity around 35 mPa·s. Its dynamic rheological response reflects its viscous nature (Figure 4a), with both moduli being strong functions of ω and G'' exceeding G' over the entire range of frequencies. At 0.01% surfactant (Figure 4b), the rheology is similar to that of the hm-chitosan alone, with a slight increase in the values of both moduli. Increasing the surfactant to 0.35% causes no dramatic changes in the rheology, with G'' still exceeding G' over the frequency range (Figure 4c). However, the slopes of G'' and G' on the frequency spectrum become nearly equal, reminiscent of the gel point rheology of a cross-linking polymer.[31] A further increase in surfactant to 0.5% induces a qualitatively different rheological response (Figure 4d). In this case, at low frequencies, G' reaches a plateau ($G' = G_0$, the gel modulus, as $\omega \rightarrow 0$), and its value exceeds that of G''. This indicates *elastic* behavior, and the lack of frequency dependence implies that the sample does not relax, that is, it has an *infinite* relaxation time. Thus, the 0.5% sample satisfies the strict rheological definition of a gel.[32]

Based on visual inspection, the 0.5% surfactant sample (Figure 4d) appears to be gel-like; however, it did not pass the tube inversion test. This suggests that the tube inversion boundary in Figure 3b is a conservative estimate and corresponds to a higher value of the gel modulus G_0 than at the onset of rheological gelation. The dynamic rheology of a "strong gel" that satisfies the tube inversion test is shown in Figure 5. This sample contains 1.4% surfactant and 0.5% hm-chitosan. In this case, the elastic modulus G' exceeds the viscous modulus G'' over the entire range of frequencies, and both moduli are frequency-independent. Note also that the "strong gel" in Figure 5 has a gel modulus G_0 of about 100 Pa, which is much higher than the G_0 of about 0.7 Pa for the weak gel in Figure 4d. Based on our rheological data, the tube inversion boundary in Figure 3b corresponds to a gel modulus of about 4 Pa. We can also approximate a boundary corresponding to the onset of gelation from the dynamic rheological data, shown by the dashed curve in Figure 3b. The two boundaries have roughly the same shape.

Figure 5 also compares the hm-chitosan and the unmodified chitosan in terms of their effect on surfactant vesicles. The dynamic rheology of two samples containing 1.4% surfactant vesicles and 0.5% polymer are contrasted. As discussed above, the hydrophobically modified polymer gives rise to a strong gel that holds its weight under tube inversion. In contrast, the unmodified chitosan merely transforms the bluish vesicle solution into a cloudy and slightly viscous fluid. The cloudiness reflects the onset of phase separation and suggests that the vesicles may be disrupted or aggregated into larger structures by the chitosan. The dynamic rheology of the chitosan sample (Figure 5) confirms its viscous behavior, with both moduli being dependent on frequency and the viscous modulus G'' exceeding the elastic modulus G'.

The contrast between the unmodified chitosan and hm-chitosan samples is further reinforced by their response under steady shear (Figure 6), where the viscosity is plotted as a function of shear rate for each case. The chitosan/vesicle mixture is a Newtonian fluid over the range of shear rates, and its viscosity is around 18 mPa·s.

(31) Winter, H. H.; Chambon, F. *J. Rheol.* **1986**, *30*, 367.
(32) Macosko, C. W. *Rheology: Principles, Measurements and Applications*; VCH Publishers: New York, 1994.

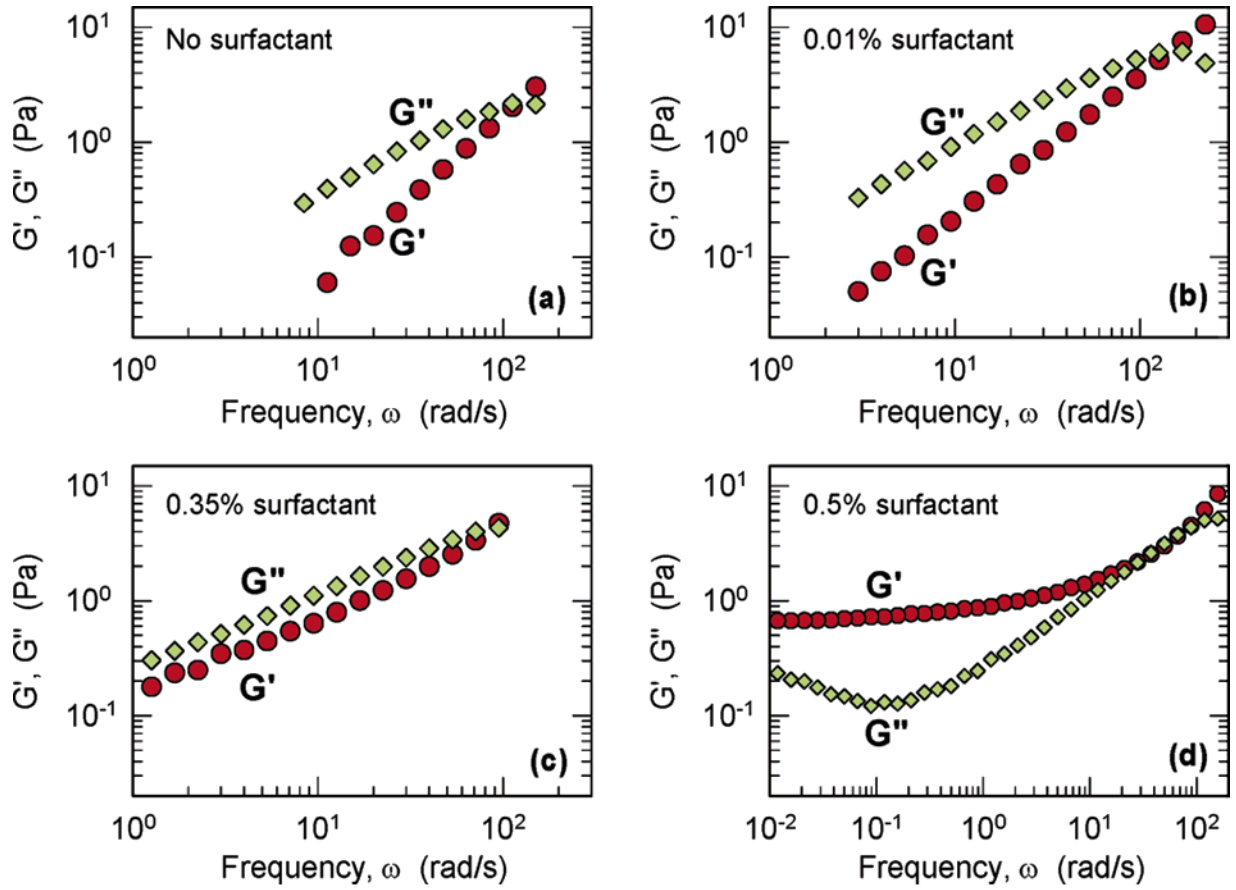

Figure 4. Dynamic rheology of vesicle−polymer mixtures as a function of surfactant content. The hm-chitosan is maintained at 0.55% and the CTAT/SDBS ratio is held fixed at 70:30 (within the vesicle region). Data are plotted for polymer (a) with no surfactant; (b) with 0.01% surfactant; (c) with 0.35% surfactant; and (d) with 0.5% surfactant. Samples a and b are viscous sols, c is close to the sol−gel transition, and d is a gel, as shown by its frequency-independent elastic modulus G' at low frequencies.

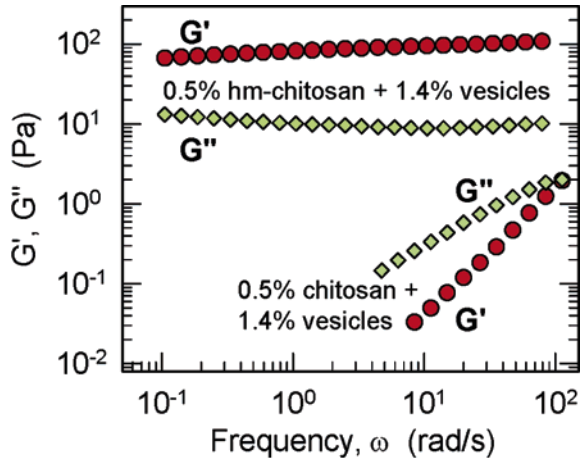

Figure 5. Comparison of the native and hydrophobically modified polymers with regard to their influence on surfactant vesicles. Dynamic rheological data are shown for two samples, each with the same vesicle concentration, that is, 1.4% CTAT/SDBS at a ratio of 70:30. One sample contains 0.5% of the native chitosan, and its rheology is that of a viscous sol. The other contains 0.5% hm-chitosan, and its rheology is that of a strong gel.

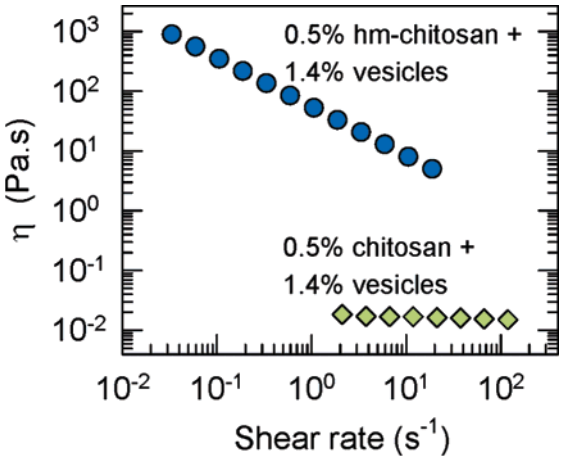

Figure 6. Comparison of the native and hydrophobically modified polymers with regard to their effect on surfactant vesicles, studied using steady-shear rheology. The apparent viscosity is plotted as a function of shear rate for the same samples studied in Figure 5.

On the other hand, the hm-chitosan/vesicle gel strongly shear-thins, and its viscosities are about 4 orders of magnitude higher. This response shows the gel-like character of the sample, with the viscosity being infinite in the limit of zero shear rate. Figures 5 and 6 show that a gel is formed only when the chitosan is hydrophobically modified.

We have studied the rheology of vesicle−polymer gels as a function of hm-chitosan and surfactant concentration (with the CTAT/SDBS ratio fixed at 70:30). In Figure 7a, the polymer is maintained at 0.55% and the gel modulus G_0 is plotted against the surfactant. Note that we tabulate G_0 only for gels, that is, for samples that show a low-frequency plateau in the elastic modulus G'. We find that G_0 sharply increases with surfactant (vesicle) concentration, the approximate relationship being $G_0 \sim c_{ves}^3$ (the best-fit line through the log−log plot in Figure 7a has a

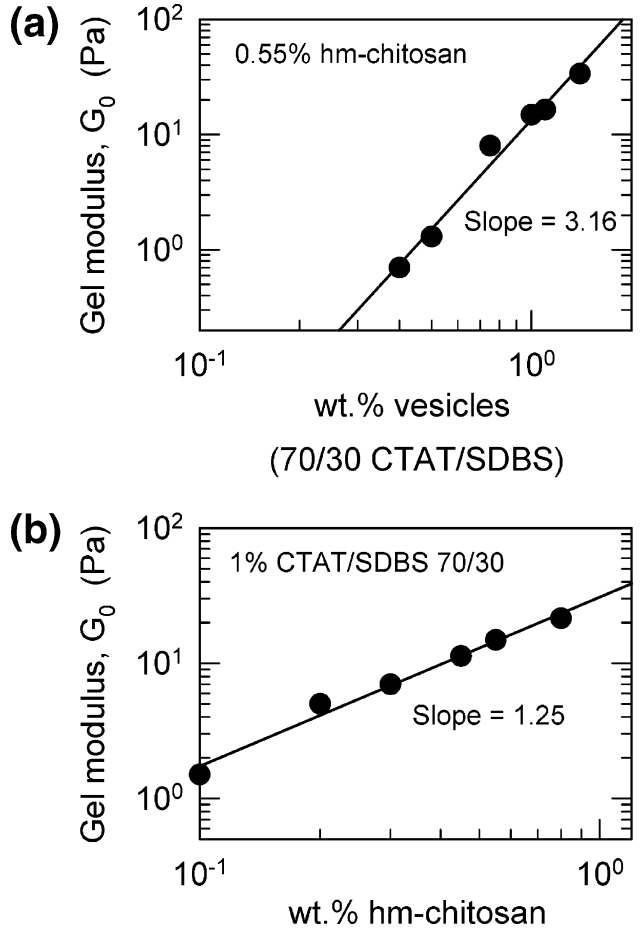

Figure 7. Gel modulus G_0 of vesicle gels formed by adding hm-chitosan to CTAT/SDBS mixtures: (a) as a function of vesicle concentration at a constant hm-chitosan concentration of 0.55%; (b) as a function of polymer concentration at a constant vesicle concentration of 1%.

slope of 3.16). In a different set of experiments, the vesicle concentration was maintained at 1% and the hm-chitosan concentration was varied. In this case, the gel modulus G_0 increases linearly with polymer concentration ($G_0 \sim c_{poly}$), as shown by the plot in Figure 7b (the best-fit slope is 1.25). The significance of these relationships will be discussed in the next section.

SANS of Vesicle−Polymer Mixtures. To probe the microstructure in our samples, we carried out SANS measurements. Samples for SANS were prepared in D_2O to achieve the needed contrast between the microstructure and the solvent. The D_2O samples were visually and rheologically identical to their counterparts made with H_2O. Figure 8 shows SANS spectra for the control vesicles (no polymer) and for a vesicle gel made by adding hm-chitosan to those vesicles. In both cases, the scattered intensity $I(q)$ shows a q^{-2} decay at moderate q, which is characteristic of bilayer scattering (eq 3). Data fits using the model for polydisperse unilamellar vesicles (eqs 4−6) are shown in Figure 8 as solid lines. From the model fit, the vesicles in the control sample (1% CTAT/SDBS at a 70:30 ratio) are seen to have an average radius R_0 of about 62 nm, with the polydispersity in the radius σ_R being about 26%. The bilayer thickness is 2.5 nm, and this can be confirmed in a model-independent fashion using a modified Guinier plot of $\ln(Iq^2)$ versus q^2 as well.[28] The parameters determined here are consistent with previous reports on CTAT/SDBS vesicles.[33]

The vesicle gel shows both the q^{-2} dependence at moderate q and the incipience of a form factor minimum

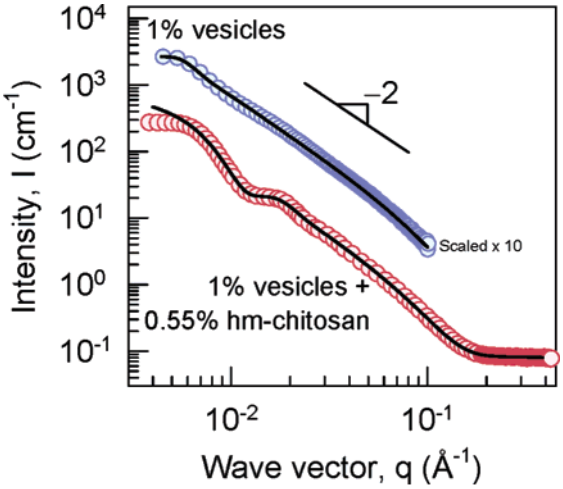

Figure 8. SANS data for a vesicle solution and the corresponding gel obtained by adding 0.55% hm-chitosan to this solution. The vesicle solution consists of 1% CTAT/SDBS at a ratio of 70:30. Both samples show the −2 slope characteristic of bilayer scattering.

at low q. This suggests that the unilamellar vesicles present in the gel are smaller than in the control case. From the model fit, we obtain an average vesicle radius R_0 of 18 nm, with the polydispersity in the radius σ_R being about 26%. The bilayer thickness is 2.5 nm as before. Note that we obtain a reasonable fit for the vesicle gel without including a structure factor $S(q)$ in the model, implying that electrostatic or excluded volume effects are not significant for the composition studied. Also, the scattering from vesicles dominates over that from the hm-chitosan in the sample, which is why we can model the data based on vesicles alone. To summarize, the key finding from Figure 8 is that the *surfactant vesicles appear to remain intact within the gel*. In addition, the vesicles in the gel appear to be significantly smaller (18-nm radius) than the control vesicles (62-nm radius).

Rheology and SANS of Wormlike Micelle−Polymer Mixtures. Our data thus far suggests that the presence of surfactant vesicles is crucial for the formation of gels with hm-chitosan. What would happen instead if we added hm-chitosan to a solution of wormlike micelles? We address this question by examining a 1% CTAT sample with no SDBS. This is a viscoelastic sample that is known to contain long, flexible wormlike micelles.[26] The elastic (G') and viscous (G'') moduli of the sample (Figure 9a) cross over at a frequency $\omega_c \approx 40\ s^{-1}$, implying a relaxation time t_R (=$1/\omega_c$) of 0.025 s. At timescales longer than t_R, the sample is a viscous fluid and its zero-shear viscosity η_0 in steady shear is 0.03 Pa·s (data not shown). When 0.55% hm-chitosan is added, the viscoelasticity is enhanced (Figure 9a). The relaxation time t_R increases to about 1 s, and the zero-shear viscosity η_0 rises to 10 Pa·s. The magnitudes of both G' and G'' are increased; however, the moduli still show a strong frequency dependence. This rheology is very different from that of the vesicle gels (compare Figures 9a and 4d). In particular, there is no plateau in G' at low frequencies, that is, at long timescales the sample is able to relax, so this is not a "true" gel. In other words, the CTAT/hm-chitosan rheology is indicative of a *transient* network formed by junctions with a *finite* timescale.

We have also used SANS to probe the microstructure in the above two samples. Figure 9b shows the $I(q)$ for 1%

(33) McKelvey, C. A.; Kaler, E. W.; Zasadzinski, J. A.; Coldren, B.; Jung, H. T. *Langmuir* **2000**, *16*, 8285.

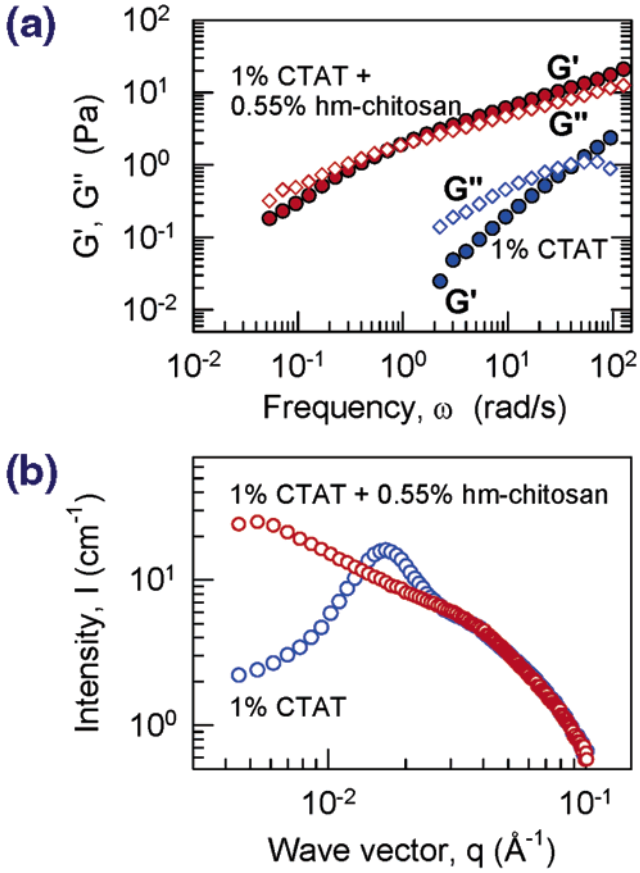

Figure 9. Comparison of a micellar solution (1% CTAT) without and with 0.55% hm-chitosan. Data from dynamic rheology (a) and SANS (b) are shown.

CTAT and for 1% CTAT + 0.55% hm-chitosan in D_2O. The 1% CTAT sample shows an interaction peak at low q (due to electrostatic repulsions between the charged micelles), but this peak disappears when hm-chitosan is added. Moreover, the two spectra overlap at high q (>0.03 Å^{-1}). In this q range, the structure factor $S(q) \rightarrow 1$, so that we can interpret the data purely in terms of a form factor. Indeed, the data in this q range are consistent with scattering from *cylindrical* micelles. The micellar radius, obtained from cross-sectional Guinier plots[28] of $\ln(Iq)$ versus q^2 (data not shown), is about 2.2 nm in both samples. This value is consistent with published data on CTAT micelles.[26] We cannot extract micellar lengths without accounting for structure factor effects, a task that is beyond the scope of the current work. However, it is interesting that micelles with the same radius exist in the presence of polymer as well.

Discussion

Our SANS data (Figures 8 and 9b) together suggest that the original surfactant microstructure dictates that observed in the presence of polymer. Taking the case of the wormlike micellar sample first, the addition of hm-chitosan enhances the viscoelasticity (Figure 9a), while retaining a *transient* network. This suggests that the network connectivity is enhanced by the binding of polymer hydrophobes to the wormlike micelles. The transient nature of the network junctions is probably related to the finite lifetime of micelles, which rapidly break and re-form over a timescale of milliseconds.[34] As a result, a polymer hydrophobe will not remain embedded in a given micelle for long; eventually, the micelle will break and release the hydrophobe, leaving it free to bind to a different micelle. The observed relaxation time of the sample (Figure 9a) will arise from a competition between two relaxation modes, one involving micelle breaking and the other involving reptation of micellar chains.[26,34]

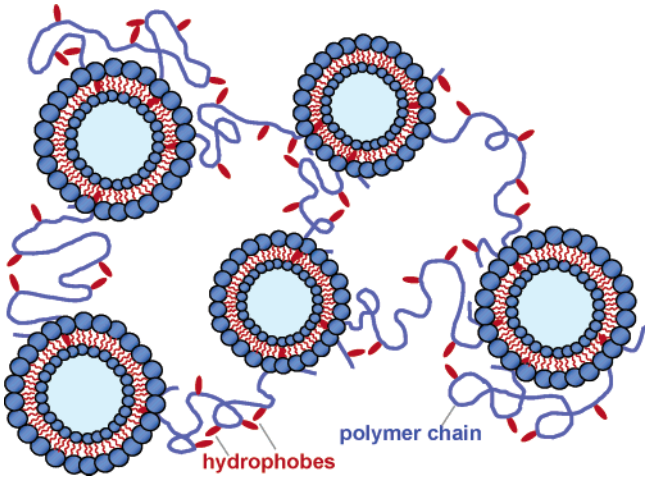

Figure 10. Proposed structure of the network formed upon addition of hm-chitosan to vesicles. Polymer hydrophobes are shown to be embedded in vesicle bilayers thus building a connected network of vesicles. Each vesicle acts as a multifunctional cross-link in the network.

Vesicle Gel Structure. In contrast to the above scenario, the addition of hm-chitosan to vesicles results in a "permanent"gel; that is, one that *does not relax* even after infinite time (Figures 4d and 5). The gel is formed only when the polymer has hydrophobes (Figure 5), and we know from SANS that the vesicles remain intact in the gel (Figure 8). Based on these findings, the likely structure of the gel is that of a network of vesicles bridged by hm-chitosan chains, as depicted in Figure 10. Here, a fraction of the polymer hydrophobes (stickers) are shown to be embedded in vesicle bilayers, so that each polymer chain is connected to two or more vesicles. The vesicles thus serve as multifunctional cross-links in a polymer gel network. The permanence of the vesicle gel is probably due to the slow rate of monomer exchange between vesicle bilayers.[35] That is, in contrast to micelles, vesicles do not break and re-form frequently, so that a hydrophobe can remain trapped in a given vesicle for a considerable period of time. Our interpretation of the vesicle gel structure coincides with that of other researchers on similar vesicle−polymer mixtures.[10−14]

To facilitate further analysis, we estimate some relevant length scales in a typical vesicle gel. Consider a 1 wt % CTAT/SDBS (70:30) mixture with 0.55 wt % hm-chitosan. Based on the vesicle size (from SANS, Figure 8) and concentration, we estimate the distance between adjacent vesicle surfaces to be about 80 nm. Taking the hm-chitosan next, the contour length of a chain of molecular weight 200 000 is about 625 nm, assuming a repeat unit size of 0.5 nm.[25] Each chain has about 25 hydrophobes, located about 25 nm apart along the chain. The reported persistence length l_p of hm-chitosan is 7.5 nm at high ionic strength,[25] which implies a radius of gyration R_g in dilute solution of 28 nm. The l_p should be higher in our samples (i.e., the chains should be more rodlike) because our ionic strength is low; thus, our R_g should also be higher.

(34) Cates, M. E.; Candau, S. J. *J. Phys.: Condens. Matter* **1990**, *2*, 6869.

(35) Evans, D. F.; Wennerstrom, H. *The Colloidal Domain: Where Physics, Chemistry, Biology, and Technology Meet*; Wiley-VCH: New York, 2001.

Additionally, for the same molecular weight, the hm-chitosan concentration at overlap c^* is reported to be about 0.1 wt %.[24,25] Beyond c^*, polymer coils overlap and begin to form "flower micelles". For $c > 10c^*$ or so, a viscoelastic network of flower micelles is expected to form, causing a sharp increase in the viscosity.[25] The viscosity of a 0.55 wt % hm-chitosan solution is relatively low (ca. 35 mPa·s, Figure 4a), so at this concentration, the polymer coils are overlapped but only weakly entangled.

Combining the above calculations, we note that in a typical vesicle gel the distance between two vesicles is much less than the contour length of an hm-chitosan chain and on the same order as its radius of gyration R_g. In such cases, the formation of polymer bridges between vesicles is indeed a plausible outcome. Theories suggest that polymer chains gain conformational entropy when vesicles are at the right distance for bridging, effectively leading to a bridging "attraction".[36−38] In this context, we assume that hydrophobes on the polymer will tend to anchor within the vesicle bilayer, and indeed this is expected to occur provided the hydrophobes are sufficiently long.[7] Moreover, in such cases, the free energy of hydrophobic interactions can overcome electrostatic repulsions between the polymer and the vesicles.[7] This explains why we observe gelation in *like-charged* (cationic) polymer and vesicle mixtures.

Our data for the onset of gelation and for the sol−gel boundary are broadly consistent with the above physical picture. Gelation occurs only above about 0.05% polymer (the asymptotic y-axis value in Figure 3b), which is close to the overlap concentration c^*. Below this concentration, the polymer is able to link a few vesicles, but there are too few chains to form a sample-spanning network. Similarly, gelation occurs only when the vesicle concentration exceeds about 0.2 wt % (the asymptotic x-axis value in Figure 3b). Below this concentration, the vesicles would be so far apart that the entropic penalty in stretching polymer chains to bridge vesicles would be excessive. Our sol−gel boundary is comparable to data reported by Porte et al.[38] for a similar class of networks, consisting of microemulsion droplets bridged by telechelic associating polymers. The "percolation line" determined by these authors has the same shape and occurs over approximately the same volume fraction range as our sol−gel line.[38] Thus, our sol−gel boundary is suggestive of a percolation threshold, corresponding to the onset of an infinite cluster of bridged vesicles.

We also observe that the vesicle size seems to be modified by the addition of hm-chitosan. Specifically, in the case of the 1% CTAT/SDBS sample (Figure 8), the vesicles become much smaller upon adding the hm-chitosan (the radius decreases from 62 to 18 nm). This, in turn, implies a sharp increase in the vesicle *number density* and, thereby, an increase in the net surface area of the vesicles. The average distance between vesicles is then reduced from about 150 nm in the control sample to 80 nm in the presence of polymer. We interpret these changes as a response of the system to promote vesicle−polymer interactions. Because the insertion of hydrophobes into vesicle bilayers is energetically favorable, the vesicles rearrange so as to present more surface area to the polymer and thereby accommodate more hydrophobes. At the same time, the reduction in intervesicle distance enables the polymer to bridge adjacent vesicles. The binding of polymer to the outer leaflet of the vesicle may also stiffen the bilayer and thereby stabilize the higher extent of curvature.

Vesicle Gel Rheology. Finally, we briefly discuss the observed trends in vesicle gel rheology. The gel modulus G_0 is a measure of the density of elastically active cross-links in the gel. We have found that G_0 increases linearly with polymer concentration c_{poly} (Figure 7b), a trend observed also by Meier et al.[11] for their vesicle gels formed with telechelic polymers. A possible interpretation is that each polymer chain binds to a certain number of vesicles, so G_0 should be proportional to c_{poly} times this number. Note that a very different scaling is expected for an entangled network of polymers or wormlike micelles, where the plateau modulus $G_p \sim c_{poly}^{2.25}$.[32] Thus, the observed linear dependence of the modulus reflects the distinctive nature of the networks studied here, where it is the vesicles that serve as junction points for the polymer chains.

We have also found that the gel modulus G_0 increases with the cube of the vesicle concentration, that is, $G_0 \sim c_{ves}^3$ (Figure 7a). The same cubic relationship has been obtained for the moduli of densely packed unilamellar[39] or multilamellar[40] vesicles. In those cases, the vesicle volume fraction was much higher and the modulus arose from the contact of individual vesicles. Here, it is the polymer chains that build the network, with the vesicles acting merely as junction points in a polymer network. The shear modulus of a semidilute polymer network is $G_0 \approx k_BT/\xi^3$, where k_BT is the thermal energy and the correlation length ξ is associated with the network mesh size.[32,34] If this relation is assumed to apply for our vesicle gels, it implies that the mesh size varies inversely with the vesicle concentration, that is, $\xi \sim 1/c_{ves}$. In other words, the mesh size decreases as more vesicles are added to the network. While this argument is appealing, further theoretical work is necessary to explore the associated ramifications.

Conclusions

In this work, we have studied mixtures of an associating biopolymer, hm-chitosan, with surfactant vesicles and wormlike micelles. We have shown that adding hm-chitosan to a vesicle solution results in an elastic gel that can hold its own weight upon tube inversion. The gels retain the bluish color that arises due to light scattering from vesicles, and SANS spectra confirm the existence of vesicles within the gel. From a rheological standpoint, the gels show a response typical of elastic solids, with frequency-independent dynamic shear moduli. The gel modulus increases linearly with polymer concentration and with the cube of the vesicle concentration. The likely structure for these gels is a network of vesicles connected by associating polymer chains, with the hydrophobes on the polymer embedded in vesicle bilayers. Upon adding the polymer, the vesicle appear to re-organize into smaller entities so as to present more surface area for interaction with the polymer hydrophobes.

Acknowledgment. This work was partially funded by NSF BES-0114790 and by a seed grant from the NSF-MRSEC at UMD. J.P.G.'s summer research was sponsored by the REU program in Molecular and Cellular Bioengineering at UMD. The authors also acknowledge NIST for facilitating the SANS experiments performed as part of this work.

LA048194+

(36) Milner, S. T.; Witten, T. A. *Macromolecules* **1992**, *25*, 5495.
(37) Lipowsky, R. *Colloids Surf., A* **1997**, *128*, 255.
(38) Filali, M.; Ouazzani, M. J.; Michel, E.; Aznar, R.; Porte, G.; Appell, J. *J. Phys. Chem. B* **2001**, *105*, 10528.
(39) Gradzielski, M.; Muller, M.; Bergmeier, M.; Hoffmann, H.; Hoinkis, E. *J. Phys. Chem. B* **1999**, *103*, 1416.
(40) Panizza, P.; Roux, D.; Vuillaume, V.; Lu, C. Y. D.; Cates, M. E. *Langmuir* **1996**, *12*, 248.